

# 000 001 002 003 004 005 006 007 008 009 010 011 012 013 014 015 016 017 018 019 020 021 022 023 024 025 026 027 028 029 030 031 032 033 034 035 036 037 038 039 040 041 042 043 044 045 046 047 048 049 050 051 052 053 PAL: PROBING AUDIO ENCODERS VIA LLMS - AUDIO INFORMATION TRANSFER INTO LLMS

Anonymous authors

Paper under double-blind review

## ABSTRACT

Integration of audio perception into large language models (LLMs) is an emerging research area for enabling machine listening applications, yet efficient transfer of rich audio semantics from audio encoders to LLMs remains underexplored. The most widely used integration paradigm projects the audio encoder output tokens into the LLM input space (e.g., via an MLP or a Q-Former), then *prepends or inserts* them to the text tokens. We refer to this generic scheme as *Prepend to the LLM's input token space (PLITS)* integration. We propose an efficient alternative, **Lightweight Audio LLM Integration (LAL)**. LAL introduces audio representations solely via the attention mechanism within different layers of the LLM, bypassing its feedforward module. LAL encodes rich audio semantics at an appropriate level of abstraction for integration into different blocks of LLMs. Our design significantly reduces computational overhead compared to existing integration approaches. Observing that Whisper style speech encoders benefit from PLITS integration, we propose an audio encoder aware approach for efficiently Probing Audio encoders via LLM (**PAL**), which in its multi encoder form employs PLITS for Whisper speech encoder and LAL for general audio encoders, and in its unified encoder form uses a single audio encoder but applies PLITS only to a compact set of speech summary tokens while integrating the full audio token sequence via LAL to preserve speech decoding capacity with low computational cost. Under an identical training curriculum, **LAL** consistently maintains performance or outperforms existing integration approaches across multiple base LLMs and tasks. For general audio tasks, LAL achieves improvements of up to 30% over a strong PLITS baseline, while reducing memory usage by about 60% and increasing throughput by about 190%. Furthermore, for general audio-music-speech LLM, **PAL**, performs on par with a fully PLITS integration-based system but with substantially improved computational and memory efficiency.

## 1 INTRODUCTION

Large Language Models (LLMs) (Brown et al., 2020; Grattafiori et al., 2024; Jiang et al., 2024; Liu et al., 2024a) have emerged as the foundational technology for natural language interaction with machines, demonstrating remarkable conversational fluency. Despite this success, their perceptual capabilities remain limited primarily to text, restricting their ability to understand the physical world. This limitation has inspired significant research into multi-modal LLMs (MLLMs), which expand traditional LLMs by integrating additional sensory modalities such as vision (Vision LLMs) (Liu et al., 2023; Templeton et al., 2024; Wang et al., 2024), audio (Large Audio Language Models (LALMs) or simply audio-LLMs) (Deshmukh et al., 2023; Gong et al., 2024; Tang et al., 2024; Ghosh et al., 2024; 2025a), and other inputs (Brohan et al., 2023; Thawkar et al., 2023) to foster more natural, intuitive, and effective human-machine interfaces.

An audio LLM typically comprises three components: (i) a large language model (LLM), (ii) one or more audio encoders, and (iii) a mechanism that integrates encoder outputs into the LLM. In this work, we investigate two such designs: a multi-encoder architecture that combines complementary encoders for general audio understanding (eg: Alex et al. (2025); Elizalde et al. (2023); Wu et al. (2023)) and speech understanding ( Radford et al. (2023)), and a unified architecture that has combined general audio speech understanding (AF-Whisper encoder in Goel et al. (2025)).

When it comes to the integration of audio encoders with the LLM, two architectural paradigms dominate today. The first transforms the outputs of an audio encoder or encoders into the LLM input space (e.g., via an MLP, a QFormer (Li et al., 2023), etc.), then *prepend* or *insert* these audio tokens to the text tokens and propagates the entire sequence through all LLM layers as if decoding jointly over audio and text. Please note that the common theme in this family is how audio tokens are passed to the LLM: they are *prepended* to the text tokens. We refer to this generic scheme **Prepend to the LLM’s input token space (PLITS)** integration, a term we have introduced to group many state of the art methods in this family of audio LLMs such as Wu et al. (2025b); Xu et al. (2025); Chu et al. (2024); Goel et al. (2025); Chu et al. (2023); Ghosh et al. (2024); Tang et al. (2024); Gong et al. (2024); Deshmukh et al. (2023). The second paradigm, **Flamingo style** architectures (Alayrac et al., 2022; Kong et al., 2024), instead insert cross attention and feedforward (FFN) blocks *between* successive LLM layers; at each insertion, text tokens attend to a set of latent audio tokens, pass through the block FFN, and only then proceed to the next LLM layer. While this design improves attention efficiency relative to PLITS concatenation, the interleaved cross attention plus FFN stacks increase sequential depth and per layer compute, which can slow the forward pass.

In contrast, we introduce **LAL**, a lightweight integration that injects audio tokens into the LLM’s attention blocks *as keys and values only* (without forming audio queries) and *bypasses the LLM FFNs for audio tokens*. This reduces the attention complexity from  $\mathcal{O}((N_a + N_t)^2)$  to  $\mathcal{O}((N_a + N_t)N_t)$ , where  $N_a$  and  $N_t$  denote the numbers of audio and text tokens, respectively. Since typically  $N_a \gg N_t$ , this yields substantial efficiency gains. By avoiding both quadratic attention over audio tokens and their passage through LLM FFNs, LAL substantially reduces memory usage and computation. Unlike parameter-efficient methods such as LoRA, this is a core architectural modification, so the efficiency benefits are realized not only during training but also at inference time.

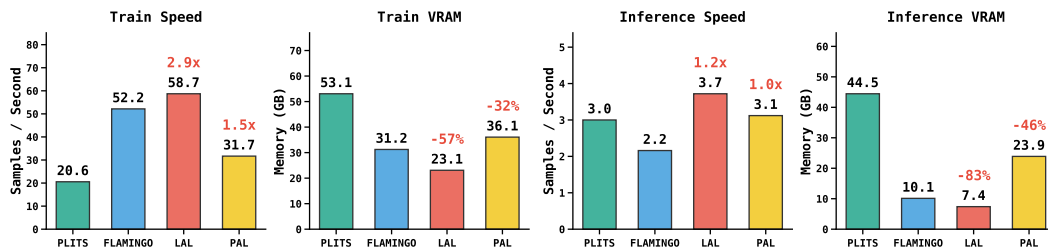


Figure 1: Comparison of compute efficiency between **PLITS**, **state of the art audio-LLM integration** (our baseline), **Flamingo**, **LAL(ours)** and **PAL(Ours)**. All use Llama3.2-1B LLM and Multi audio encoder setup (ref to Section 3.3.1). Training was performed with batch size 8 on an NVIDIA A100 using bfloat16, and inference with batch size 12 on an NVIDIA A100 using float16. All benchmarks were executed sequentially on the same node to eliminate load-related discrepancies.

LAL provides a compute and memory-efficient mechanism by constraining how audio tokens interact with the LLM. However, some modalities, especially speech, which closely mirrors text, may benefit from the richer token-level decoding of PLITS-style integration. Motivated by this observation, we introduce two hybrid variants that combine LAL and PLITS, one in the multi audio encoder setting and one in the unified audio encoder setting. We refer to this family as the PAL framework for building general purpose audio, music, and speech LLMs, enabling fusion that balances efficiency and performance. This design achieves strong results while substantially reducing computational and memory requirements compared to using PLITS style integration alone.

To validate these architectural choices, we conduct a systematic empirical study under a standardized training curriculum and dataset setup, ensuring fair comparisons across models. Our experiments explore the trade-off between performance and efficiency, highlighting how different integration techniques facilitate effective information transfer from audio encoders to LLMs with minimal parameter overhead. This analysis provides actionable insights into the design of scalable and efficient audio LLMs that leverage diverse pretrained audio encoders.

**Our main contributions are as follows:** (1) We introduce **LAL**, a lightweight integration strategy for audio-LLMs that incorporates audio tokens solely as keys and values in the LLM’s attention sub-modules and skips FFNs, thereby reducing computation and memory cost while retaining

108 performance comparable to PLITS integration, **(2)** Motivated by the observation that speech un-  
 109 derstanding benefits from PLITS integration, we propose **PAL**, a hybrid integrated LLM. In the  
 110 multi encoder setup, PAL is encoder aware and selectively applies LAL or PLITS based on the  
 111 audio encoder, while in the unified encoder setup it applies PLITS to a summarized subset of to-  
 112 kens and LAL to all tokens, enabling general purpose audio, speech, and music LLMs that balance  
 113 efficiency and performance, and **(3)** We conduct **fair and rigorous architectural comparisons**  
 114 under a standardized training curriculum and dataset setup, providing actionable insights into the  
 115 efficiency–performance trade-offs of audio-LLM design.

116

## 117 2 LITERATURE REVIEW

118

119 **Audio LLM architectures:** When integrating audio encoders with an LLM, two paradigms dom-  
 120 inate. In PLITS, encoder features are mapped to the LLM token space with a small projector such  
 121 as an MLP or a Q Former, the resulting audio tokens are typically prepended to the text tokens, and  
 122 the joint sequence is processed by all LLM layers (Wu et al., 2025b; Xu et al., 2025; Chu et al.,  
 123 2024; Goel et al., 2025; Chu et al., 2023; Ghosh et al., 2024; Tang et al., 2024; Gong et al., 2024;  
 124 Deshmukh et al., 2023). In contrast, the Flamingo style architecture inserts cross attention and feed  
 125 forward adapters between successive LLM layers so that text tokens attend to latent audio tokens  
 126 at selected depths (Alayrac et al., 2022; Kong et al., 2024). This makes audio to text interaction  
 127 explicit and gated, but adds sequential depth, per layer compute, and parameters.

128

129 **Audio-LLM Datasets:** Beyond architecture, recent works have focused on high-quality instruction  
 130 tuning datasets, both open-source and proprietary (Goel et al., 2025; Ghosh et al., 2024; Chu et al.,  
 131 2024; Xu et al., 2025) and build audio reasoning benchmarks (Sakshi et al., 2024; Deshmukh et al.,  
 132 2025a;b). Training PLITS or Flamingo-style models on these resources improves instruction fol-  
 133 lowing and audio reasoning, with most gains driven by the data rather than the integration scheme.

134

## 135 3 METHODOLOGY

136

137 This section outlines our approach to integrating audio with language models. We begin by formal-  
 138 izing **PLITS**, the SOTA audio-LLM integration, as our reference baseline. We then introduce **LAL**,  
 139 a lightweight alternative that injects audio through attention only, and we analyze its compute and  
 140 memory profile. Finally, we connect these findings to **PAL**, an encoder aware hybrid that selects  
 141 between PLITS and LAL on a per encoder basis in order to support speech understanding without  
 142 sacrificing efficiency on general audio.

143

### 3.1 BASELINE AUDIO LLM: PREPEND TO THE LLM’S INPUT TOKEN SPACE (PLITS)

144

145 To provide a fair comparison point for our integration methods, we construct a baseline audio LLM  
 146 that follows the widely adopted SOTA integration strategy, which we refer to as *Prepend to the*  
 147 *LLM’s input token space (PLITS)*. In this design, the audio encoder outputs are first mapped into  
 148 the LLM input embedding space using a Q-Former-style connector. The resulting audio tokens are  
 149 then *prepended* to the text tokens, and the concatenated sequence is passed through all LLM layers  
 150 so that decoding proceeds jointly over audio and text (see Fig. 2(A)).

151

152 The central characteristic of this PLITS-style integration is that **the audio tokens are prepended to**  
 153 **the text tokens**. This integration strategy is used by most audio LLMs, including several state of  
 154 the art systems Wu et al. (2025b); Xu et al. (2025); Chu et al. (2024); Goel et al. (2025); Chu et al.  
 155 (2023); Ghosh et al. (2024); Tang et al. (2024); Gong et al. (2024); Deshmukh et al. (2023).

156

### 157 3.2 LAL: LIGHTWEIGHT AUDIO-LLM INTEGRATION

158

159 Recent work in mechanistic interpretability suggests that LLMs encode semantics as features that  
 160 can be selectively activated within hidden states (Elhage et al., 2022; Bricken et al., 2023; Templeton  
 161 et al., 2024). Building on this view, we hypothesize that effective audio LLM integration requires  
 162 audio tokens to trigger the activation of sound related conceptual features inside the textual token  
 163 embeddings. In other words, distinct auditory inputs should induce the corresponding linguistic con-  
 164 cepts to become active in the text representation; for example, when the input contains a *dog bark*,

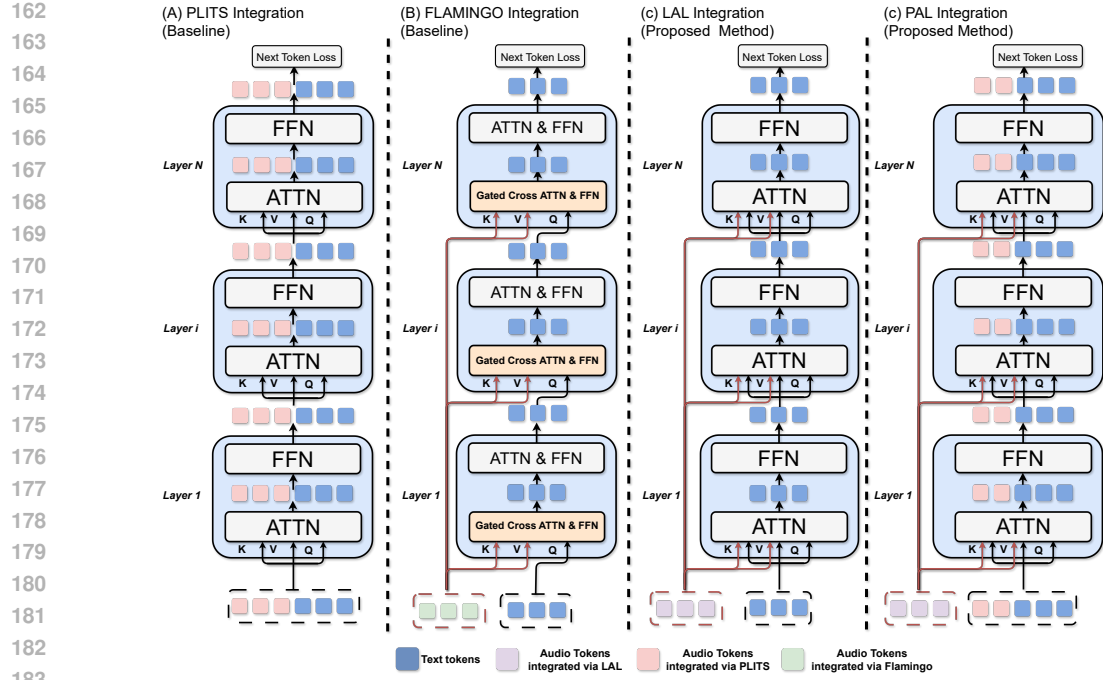


Figure 2: Illustration of integration techniques: (A) SOTA integration **PLITS** (prepend to the LLM’s input token space), which prepends audio tokens to text tokens and propagates the full sequence through all LLM layers (our baseline); (B) **Flamingo** integration, where text tokens first attend to audio tokens through a separate cross attention plus FFN module, and the resulting signal is added to the text residual stream before the next LLM layer. (C) our proposed lightweight integration **LAL**, which introduces audio representations only through the attention mechanism (see Equations 2, 3, and 4) while bypassing the feedforward modules; (C) the hybrid **PAL**, an encoder aware/hybrid integration that combines **LAL** and **PLITS** integrations.

the features associated with the concept *dog* should light up so the model can ground the auditory signal in language and answer queries such as *Which animal sound is present?*. This hypothesis guides our architectural design: we seek the simplest pathway that reliably transmits audio cues into the text features that carry concepts.

A standard LLM layer consists of an attention submodule followed by a feed-forward network (FFN) submodule. Since attention mediates all inter-token interactions, it is the necessary pathway for audio to influence text, and we posit that it is also sufficient for text tokens to gather information from audio. Guided by this principle, we introduce **LAL** (Lightweight Audio LLM integration).

As in our baseline, a shared Q-Former produces a sequence of audio tokens and at each layer a small MLP projects these tokens into that layer’s input space. Audio information is then injected into the attention block only through Keys and Values while Queries remain text only, so audio modulates the attention context of text tokens without passing through the feed-forward network.

Formally, let  $H_l^t \in \mathbb{R}^{N_t \times d}$  denote the text hidden states at layer  $l$  and  $A \in \mathbb{R}^{N_a \times d_a}$  the Q-Former audio features. A per-layer projector  $P_l : \mathbb{R}^{d_a} \rightarrow \mathbb{R}^d$  maps audio to the layer space,

$$\hat{A}_l = P_l(A) \in \mathbb{R}^{N_a \times d} \quad (1)$$

and we concatenate text and audio along the token axis

$$S_l = [H_l^t; \hat{A}_l] \in \mathbb{R}^{(N_t + N_a) \times d}. \quad (2)$$

216 Queries are formed from *text only* (see Figure 2(B)), while Keys and Values are computed from the  
 217 concatenated sequence:

$$219 \quad Q_l^t = H_l^t W_{Q,l}, \quad K_l = S_l W_{K,l}, \quad V_l = S_l W_{V,l}. \quad (3)$$

221 The resulting LAL update for text tokens is

$$223 \quad \tilde{H}_l^t = \text{softmax}\left(\frac{Q_l^t K_l^\top}{\sqrt{d_k}}\right) V_l. \quad (4)$$

226 after which  $\tilde{H}_l^t$  proceeds through the FFN with the usual residual connections. In this way, au-  
 227 dio cues shape the attention context seen by text tokens, aligning audio-evoked features with their  
 228 linguistic counterparts and enabling effective cross-modal information transfer.

229 **Information Injection Dynamics. LAL is neither Lite PLITS nor Lite Flamingo.** Beyond com-  
 230 putational efficiency, LAL opens up a distinct information pathway. In PLITS, audio tokens are  
 231 treated identically to text tokens: they are transformed layer by layer through causal self-attention  
 232 and FFN non-linearities, causing their representations to drift from the original encoder output as  
 233 they mix with the LLM’s internal state. In contrast, LAL uses a dedicated MLP at each layer to  
 234 project “semantic-ready” audio features directly into the appropriate abstraction for that layer. This  
 235 preserves a direct link to the audio encoder’s semantic output. For tasks that rely on explicit acoustic  
 236 cues, such as sound event understanding (e.g., *Which animal sound is heard?*), this projection-based  
 237 injection can be more effective than the deeply transformed representations produced by PLITS.

238 When comparing to Flamingo, we note that although Flamingo also injects semantic level information  
 239 without decoding audio tokens inside the LLM, the route by which this information influences  
 240 text tokens is fundamentally different. In Flamingo, text tokens first attend to audio tokens in a dedi-  
 241 cated cross attention module; the resulting signal is added to the text residual stream, and only then  
 242 do the updated text states interact through the standard self attention layers of the LLM. In LAL,  
 243 by contrast, audio representations are introduced directly into the same self attention operation as  
 244 the text tokens, so text attends jointly to audio and text within a single attention computation. This  
 245 produces a distinct information flow from Flamingo. We also note that LAL does not require the  
 246 extra cross attention plus FFN adapter blocks used in Flamingo.

247 To summarize, LAL is similar to PLITS in that it performs in-context injection and allows text tokens  
 248 to attend over both audio and text tokens, and it is similar to Flamingo in that it injects information  
 249 that has not been fully decoded inside the LLM. However, it is architecturally distinct from both:  
 250 LAL is neither a “lite PLITS” nor a “lite Flamingo,” but rather a new information pathway for  
 251 integrating audio encoders with LLMs.

252 **LAL Integration with Frozen LLM FFN.** We also verify that LAL integration remains effec-  
 253 tive when the LLM’s FFN blocks are frozen, with no significant loss in performance (refer to Ap-  
 254 pendix E). This finding has important implications for reducing training cost, improving parameter  
 255 efficiency, and preserving the pretrained knowledge of the LLM while enabling multimodal align-  
 256 ment. For clarity and consistency, however, our main experiments focus on the standard setting with  
 257 trainable FFN blocks, and discussion of the frozen-FFN variant is limited to Appendix E.

258 **Leveraging parametric versus contextual knowledge.** Here we posit how LAL *efficiently* util-  
 259 izes two types of knowledge inherent in pre-trained LLMs: (1) parametric knowledge, primarily  
 260 embedded within the FFN layers as a result of extensive language pre-training, and (2) contextual  
 261 knowledge, which is dynamically incorporated through attention mechanisms. We posit that audio  
 262 as contextual information can effectively induce required concept activations in text token repres-  
 263 entations via attention-based modulation, without needing direct FFN processing of audio repres-  
 264 entations. Consequently, audio information indirectly accesses the LLM’s parametric knowledge: the  
 265 audio context “piggybacks” on text tokens, as attention mechanisms reconfigure these repres-  
 266 entations, which then engage relevant concept-related pathways during FFN processing.

### 267 3.2.1 COMPUTE AND MEMORY EFFICIENCY.

268 LAL is more compute- and memory-efficient than PLITS and Flamingo style integration, and the  
 269 benefits become more pronounced with longer audio sequences. At a high level, the gains come

270 from reducing the effective attention complexity and avoiding unnecessary routing of audio tokens  
 271 through the feed-forward sublayers. Quantitative comparisons of memory usage and training  
 272 throughput are reported in Figure 1.

273 In the following subsections, we present one-to-one comparisons between LAL and the PLITS base-  
 274 line when applicable, and otherwise discuss properties specific to LAL.  
 275

276 **Attention Complexity:**

277 *PLITS*: full causal attention over  $N_a + N_t$  tokens with cost  $\mathcal{O}((N_a + N_t)^2)$   
 278

279 *LAL*: only text tokens issue queries; keys and values include audio and text, with cost  
 280  $\mathcal{O}((N_a + N_t)N_t)$  eliminating the  $N_a^2$  term and all audio to audio interactions.  
 281

282 **Feedforward Routing:**

283 *PLITS*: audio tokens pass through attention and the feedforward sublayer in every block, increasing  
 284 floating point operations and activation memory in proportion to  $N_a$ .  
 285

286 *LAL*: audio tokens do not enter the feedforward sublayer and only serve as keys and values for text  
 287 queries, which reduces per layer floating point operations and activations stored for backpropagation.  
 288

289 **Scaling With Audio Length:** Non text modalities in multimodal LLMs often yield far more tokens,  
 290 and audio is no exception. As  $N_a$  grows due to longer clips or denser tokenization, PLITS incurs  
 291 a cost of  $(N_a + N_t)^2$ , so the  $N_a^2$  term dominates. In contrast, LAL scales as  $(N_a + N_t)N_t$ , which  
 292 is linear in  $N_a$ . Thus, the compute and memory gap widens with longer or more finely segmented  
 293 audio. The feedforward savings in LAL also increase with  $N_a$  as a larger share of tokens bypass the  
 294 most expensive part of each block.  
 295

296 **Distinct from PEFT and LoRA:** LAL is a core architectural modification, not a parameter-efficient  
 297 fine-tuning (PEFT) method such as LoRA (Hu et al., 2022). Techniques such as LoRA adjust how  
 298 weights are adapted during training while keeping the forward compute pattern essentially the same  
 299 at inference. In contrast, LAL changes how audio tokens participate in attention and feedforward  
 300 routing, so its compute and memory savings apply at inference as well as during training.  
 301

302 **3.3 PAL: ADDING SPEECH UNDERSTANDING**

303 Speech occupies a special position among audio modalities because it is closely tied to language and  
 304 is often described simply as spoken language. In Whisper style systems, speech encoders are trained  
 305 with transcription style or next text token prediction objectives, so their internal representations form  
 306 sequences that already resemble linguistic tokens. It is therefore beneficial to use PLITS integration  
 307 for speech, since this strategy allows the model to decode spoken language in the same space where  
 308 it already reasons over text and leads to better extraction of speech information.  
 309

310 In contrast, general audio encoders trained with self supervised or contrastive objectives are opti-  
 311 mized to produce high level semantic descriptors or event level features rather than language like  
 312 sequences. For these encoders, it is often sufficient for text tokens to attend to audio features in order  
 313 to retrieve the relevant information, without requiring the audio tokens themselves to be processed  
 314 by the LLM feed forward layers. LAL offers a more efficient integration path in this setting because  
 315 audio tokens appear only as keys and values in attention while the LLM feed forward blocks operate  
 316 solely on text representations.  
 317

318 This separation is also consistent with classical neuro linguistics: Wernicke’s area is primarily as-  
 319 sociated with comprehension of spoken and written language, while the angular gyrus supports  
 320 association across auditory, visual, and other sensory inputs. By analogy, speech features may be  
 321 most effective when interpreted inside a language centric pathway, whereas general audio benefits  
 322 from a more modality specific route. Empirically, we observe that speech understanding gains from  
 323 PLITS style decoding inside the LLM for speech encoders such as Whisper. Building an efficient  
 324 LLM that understands both speech and general audio therefore requires an appropriate allocation  
 325 of integration strategies between LAL and PLITS. Within our PAL framework, we instantiate this  
 326 idea in two variants: PAL-MultiEnc (Section 3.3.1), where separate encoders for general audio and  
 327 for speech are each integrated with the LLM, and PAL-UniEnc (Section 3.3.2), a unified encoder  
 328 model in which a single audio encoder supports both speech and general audio and interfaces with  
 329 the LLM.  
 330

324 3.3.1 MULTI AUDIO ENCODER PAL  
325

326 In the multi-encoder PAL architecture, we combine complementary encoders for general audio and  
327 speech. General audio encoders such as CLAP and SSLAM provide tokens that capture language  
328 aligned semantics and fine grained acoustic detail. These tokens are integrated into the LLM through  
329 LAL, so they serve as keys and values in the attention blocks without entering the feed forward  
330 pathways.

331 Speech is handled by a dedicated encoder such as Whisper. The Whisper tokens are mapped into  
332 the LLM input space and integrated through the PLITS pathway, where they are prepended to text  
333 tokens and processed as full tokens by all LLM layers(Figure 4). This encoder aware allocation  
334 allows PAL to use the efficient LAL integration for general audio while reserving compute intensive  
335 PLITS integration for speech. We refer to this model as PAL/LAL/PLITS-MULTIENC.

336 3.3.2 UNIFIED AUDIO ENCODER PAL  
337

338 In the unified encoder PAL architecture, we use AFWhisper Goel et al. (2025) as a single audio en-  
339 coder that supports both speech and general audio understanding. AFWhisper produces a sequence  
340 of audio tokens for each input clip. To balance efficiency with the benefits of PLITS for speech like  
341 content, we construct two parallel views of this sequence.

342 First, we derive a compact set of summary tokens by applying a one dimensional convolution with  
343 stride  $r$  along the time axis, which reduces the token count by a factor of  $r$ . These summary tokens  
344 are treated as PLITS tokens: they are mapped into the LLM input space, prepended to the text  
345 tokens, and processed as full tokens through all LLM layers.

346 Second, we retain the complete AFWhisper token sequence for LAL integration. In each attention  
347 block, audio information enters as keys and values via these full resolution tokens and the audio  
348 summary tokens integrated via PLITS, while queries are issued by text tokens and summary tokens.  
349 To preserve temporal ordering, we interleave the tokens in attention(in key and value) so that, within  
350 each span of  $r$  original AFWhisper tokens, the corresponding summary token is placed after its  
351 source tokens (see Figure 5). Concretely, the ordering of keys and values in the attention module  
352 follows

$$z = (\ell_1, \ell_2, \dots, \ell_r, p_1, \ell_{r+1}, \dots, \ell_{2r}, p_2, \dots), \quad (5)$$

353 where  $\ell_i$  denotes an LAL token and  $p_j$  denotes a summary token that is integrated via PLITS. This  
354 maintains the alignment between summary tokens and their underlying fine grained audio context.  
355

356 In this way, unified PAL allows the model to benefit from PLITS style decoding over a compact set  
357 of audio summaries while still exposing the full AFWhisper token sequence to LAL based atten-  
358 tion. We refer to this model as PAL/LAL/PLITS-UNIENC. Additional details such as, visualiza-  
359 tion(Figure 4), ablations 10 are provided in Appendix E.2.

361 4 EXPERIMENTS AND RESULTS  
362

363 We empirically evaluate our audio-language framework on a range of audio understanding and rea-  
364 soning tasks. Unless otherwise specified, we use Llama 3.2 1B Instruct (Grattafiori et al., 2024)  
365 as the base LLM. For larger backbones, we report results with Llama 3.2 3B Instruct (Grattafiori  
366 et al., 2024), and to assess transfer across model families, we additionally evaluate Qwen2.5 1.5B  
367 Instruct (Team, 2024). For audio encoders, we employ SSLAM and CLAP connected via an efficient  
368 Q-former-based module that combines their representations without increasing the token count, in-  
369 spired by Tong et al. (2024); we refer to this connector as **LFST**. We use LFST for all multi encoder  
370 experiments unless otherwise specified. In experiments where LFST is not used, we use SSLAM  
371 encoder. See Appendix E.1 for further details on **LFST**.

372 In the following subsections, we present the training setups and results for LAL and PAL.

373 4.1 LAL  
374

375 **Training Protocol.** We train the proposed audio LLM variants on the one of the largest general  
376 audio instruction tuning datasets OpenAQA dataset (Gong et al., 2024) and CompA-R Ghosh et al.

(2024). Our two-stage pipeline comprises: (i) connector pretraining, where only the connector is trained and all other modules are frozen; and (ii) joint training of the connector and the LLM. The audio encoders remain frozen throughout.

For reasoning and open ended question answering we additionally train on open ended data from OpenAQA Gong et al. (2024) as Stage 3 and on the reasoning dataset CompA R Ghosh et al. (2024) as Stage 4. Additional training details are in Appendix C.1.

**Evaluation Protocol.** To assess how effectively LAL transfers critical audio-event information from the encoder to the LLM’s latent space, we evaluate on downstream classification, captioning, and reasoning tasks. Following the LTU framework (Gong et al., 2024): (i) for classification, we measure semantic similarity by encoding both model text outputs and target audio labels with `gpt-text-embedding-ada`; (ii) for captioning, we use standard audio captioning datasets and report CIDEr and SPICE.

For reasoning, we adopt the compA-R-test and the evaluation protocol of (Ghosh et al., 2024): we prompt a text-only GPT-4 judge with the audio-LLM’s output and auxiliary metadata about the audio events, and obtain scores for *Helpfulness*, *Clarity*, *Correctness*, *Depth*, and *Engagement*. Additional evaluation details are in Appendix D.1.

**Results** To clearly separate contributions, we present two sets of results. First, in Table 1 (classification and captioning) and Table 2 (reasoning), we report a controlled comparison between LAL, Flamingo and PLITS, showing that LAL achieves comparable or better accuracy while being more efficient in speed and memory. Second, in Table 3 (classification and captioning) and Table 4 (reasoning), we compare LAL with prior works. Note that training data scale and model size vary significantly across prior approaches; our model operates on the lower end of both dimensions. These results should therefore be interpreted as evidence that LAL remains competitive despite using fewer resources.

Table 1: Performance evaluation of the proposed efficient integration method **LAL** and SOTA integration **PLITS** across different base LLMs. Evaluation follows the protocol of Gong et al. (2024). FI:Flamingo Integration, AC: Audio caps, CL:Clotho AS2M: AudioSet 2M <sup>†</sup> indicates CIDEr and <sup>‡</sup> indicates SPICE. Other metrics: accuracy (ESC-50, VocalSound), Mi-F1 (DCASE), and mAP (FSD, AudioSet). For evaluation methodology see Section 4.1 and for dataset details see Appendix D

LLM	PLITS	FI	LAL	LFST	Classification					Captioning				
					Backbone	ESC50	DCASE	VS	FSD	AS2M	AC <sup>†</sup>	CL <sup>†</sup>	AC <sup>‡</sup>	CL <sup>‡</sup>
Llama3.2-1B		✓	✗	✗	✗	64.45	37.69	51.57	25.23	9.08	0.59	0.34	16.30	10.96
		✗	✗	✓	✗	76.70	40.97	<b>60.87</b>	31.44	11.83	0.66	0.38	16.97	11.87
		✓	✗	✗	✓	84.10	45.28	57.59	42.49	14.74	0.70	0.39	17.90	11.82
		✗	✓	✗	✓	84.95	43.95	55.44	41.27	<b>15.0</b>	0.69	0.39	17.09	11.91
		✗	✗	✓	✓	<b>87.40</b>	<b>46.23</b>	56.03	<b>43.91</b>	14.74	<b>0.72</b>	<b>0.42</b>	<b>18.08</b>	<b>12.58</b>
Llama3.2-3B		✓	✗	✗	✗	70.40	40.62	61.40	28.88	10.84	0.63	0.35	16.81	11.35
		✗	✗	✓	✗	82.15	43.21	<b>65.78</b>	34.29	12.91	0.67	0.38	17.80	12.18
		✓	✗	✗	✓	84.60	46.16	59.15	43.29	15.00	0.7	0.38	17.9	12.03
		✗	✗	✓	✓	<b>89.25</b>	<b>47.21</b>	60.46	<b>43.86</b>	<b>15.03</b>	<b>0.73</b>	<b>0.40</b>	<b>18.61</b>	<b>12.46</b>
Qwen2.5-1.5B		✓	✗	✗	✗	68.00	37.57	56.45	27.87	9.56	0.63	0.38	16.63	11.74
		✗	✗	✓	✗	70.85	38.79	<b>59.20</b>	28.53	10.28	0.63	0.38	16.65	11.44
		✗	✗	✓	✓	<b>87.80</b>	<b>45.52</b>	56.73	<b>43.26</b>	<b>13.92</b>	<b>0.73</b>	<b>0.41</b>	<b>18.45</b>	<b>12.20</b>

Table 2: GPT-4 evaluation of LAL and PLITS on the CompA-R benchmark (Ghosh et al., 2024). A text only GPT-4 judge scores the model outputs; see Ghosh et al. (2024) for the detailed prompt.

PLITS	LAL	LFST	Helpfulness	Clarity	Correctness	Depth	Engagement
✓	✗	✓	<b>3.86</b>	<b>4.74</b>	<b>3.84</b>	2.86	2.99
✗	✓	✓	3.85	4.70	3.82	<b>2.88</b>	<b>3.01</b>

## 4.2 PAL

**Training Protocol.** PAL follows the same two stage procedure as LAL: (i) connector pretraining, where only the connector is trained and all other modules are frozen; and (ii) joint training of the

432  
 433 Table 3: Comparison of LAL classification and captioning performance with prior works. Except  
 434 for Audio Flamingo 2, all other systems use PLITS; their higher scores mainly stem from larger  
 435 datasets, bigger LLMs, and stronger audio encoders.

436 437 Models	Classification					Captioning			
	438 ESC50	439 DCASE	440 VS	441 FSD	442 AS2M	443 AC <sup>†</sup>	444 CL <sup>†</sup>	445 AC <sup>‡</sup>	446 CL <sup>‡</sup>
Pengi-124M	<b>91.9</b>	33.8	60.3	46.7	-	-	-	-	-
SALMONN-7B	16.4	18.0	16.9	22.1	13.4	-	-	8.3	7.6
Audio Flamingo-2-3B	83.9	-	-	<b>47.9</b>	-	0.58	<b>0.46</b>	-	-
LTU-7B	83.1	45.9	55.6	46.3	18.7	-	-	17	11.9
GAMA-7B	82.6	38.4	52.4	47.8	<b>19.2</b>	-	-	18.5	13.5
LAL-1B (Ours)	87.40	46.23	56.03	43.91	14.74	0.72	0.42	18.08	12.58
LAL-3B (Ours)	89.25	<b>47.21</b>	<b>60.46</b>	43.86	15.03	<b>0.73</b>	0.40	<b>18.61</b>	12.46

447 Table 4: LAL performance comparison with prior works for the reasoning (CompA-R) task. All  
 448 prior works use PLITS integration. Their higher scores mainly stem from larger datasets, bigger  
 449 LLMs, and stronger audio encoders.

450 451 452 453 454 455 Models	456 Clarity	457 Correctness	458 Engagement	459 Avg
Qwen-Audio-Chat-8B (Chu et al., 2023)	3.5	3.3	3.6	3.5
LTU-7B (Gong et al., 2024)	3.5	3.2	3.4	3.4
SALMONN-7B (Tang et al., 2024)	2.6	2.4	2.0	2.3
Pengi-124M (Deshmukh et al., 2023)	1.8	1.5	1.3	1.5
LTU w/ CompA-R-7B (Gong et al., 2024)	3.5	3.2	3.4	3.6
GAMA-IT-7B (Ghosh et al., 2024)	4.3	<b>3.9</b>	<b>3.9</b>	<b>4.0</b>
LAL-1B (Ours)	<b>4.70</b>	3.82	3.01	3.80

460 connector and the LLM. The audio encoders remain frozen throughout. For Stage 1, we construct  
 461 a mixture from the general audio OpenAQA Stage 1 set, augmented with the OpenASQA (Gong  
 462 et al., 2023b) Stage 1 split for speech understanding. For Stage 2, we use a curated audio, speech,  
 463 and music reasoning instruction tuning corpus, specifically a 6M subset of AudioSkills (Goel et al.,  
 464 2025).

465 **Evaluation Protocol.** We first target speech understanding with two tasks: speech recognition  
 466 and speaker gender classification (using `gpt-text-embedding-ada` as explained in Section  
 467 4.1); We then assess general audio, music, and speech reasoning on MMAR Ma et al. (2025),  
 468 MMAU Sakshi et al. (2024) and MMSU Wang et al. (2025) which report detailed category wise  
 469 performance.

470 **Results.** Our experiments on the speech understanding and reasoning benchmark MMSU(Table 12)  
 471 (refer to Appendix E.3), speech based emotion recognition, gender classification (Table 11) and  
 472 the speech subsets in MMAU (Table 5) and MMAR (Table 6) show that LAL consistently exhibits  
 473 reduced performance compared to PLITS on speech based tasks. This substantiates the need for the  
 474 hybrid PAL architecture.

475 From our evaluation results in Table 11 for classification and Tables 5 and 6 for reasoning, PAL is  
 476 comparable to PLITS in accuracy while retaining efficiency advantages in both multi encoder and  
 477 unified encoder setups. In the multi encoder setup, we also observe that adding a Whisper encoder  
 478 changes performance in the general audio (sound) and music domains. We hypothesize that this is  
 479 because Whisper encodes background sounds, as reported by Gong et al. (2023a), which provides  
 480 some event detection capability.

481 Our PAL versus PLITS comparison is controlled within our setup, using the same backbone, data,  
 482 and training hyperparameters; see Appendix C.2 for details. The primary comparison in these tables  
 483 is therefore between PAL, LAL and PLITS, and results from prior work are included only to place  
 484 PAL in the broader literature. With the exception of Audio Flamingo 2, the other systems are based  
 485 on PLITS. The higher scores reported by some prior systems over our PLITS baseline largely reflect  
 486 larger training sets, larger LLMs, and stronger audio encoders. This work assesses the integration in  
 487 isolation, which is why we focus on the PAL versus PLITS comparison.

486  
 487 Table 5: Evaluation on **MMAU-v05.15.25** (Sakshi et al., 2024) (accuracy, %). Sound (Sn), Music  
 488 (Mu), Speech (Sp), and r (reduction factor, Section 3.3.2). Except for Audio Flamingo 2, all other  
 489 systems use PLITS; their higher scores mainly stem from larger datasets, bigger LLMs, and stronger  
 490 audio encoders. **Boldface** marks PAL multi encoder and unified encoder variants separately, reflect-  
 491 ing our focus on integration.

492	Model	Sn		Mu		Sp		Total (Avg)							
		493	mini	494	mini	495	mini	496	497	test	498	test	499	test	500
493	Step-Audio-2-mini-8.3B (Wu et al., 2025a)	79.30	75.57	494	68.44	495	66.85	496	66.18	497	66.49	498	72.73	499	70.23
494	DeSTA2.5-Audio-8B (Lu et al., 2025)	70.27	66.83	495	56.29	496	57.10	497	71.47	498	71.94	499	66.00	500	65.21
495	SALMONN-13B (Tang et al., 2024)	41.14	42.10	496	37.13	497	37.83	498	26.43	499	28.77	500	34.90	36.23	
496	GAMA-7B (Ghosh et al., 2024)	31.83	30.73	497	17.71	498	17.33	499	12.91	500	16.97	31.82	21.68		
497	GAMA-IT-7B (Ghosh et al., 2024)	30.93	32.73	498	26.74	499	22.37	500	10.81	31.74	497	11.57	22.83	22.22	
498	LTU-7B (Gong et al., 2024)	20.42	20.67	499	15.97	500	15.68	31.74	497	15.92	498	15.33	17.44	17.23	
499	Qwen2.5-Omni-7B (Xu et al., 2025)	78.10	76.77	500	65.90	31.74	67.33	31.74	497	70.60	498	68.90	31.74	71.50	71.00
500	Qwen2-Audio-Instruct-7B (Chu et al., 2024)	67.27	61.17	501	56.29	502	56.29	503	55.67	504	55.57	505	59.90	506	57.40
501	M2UGen-7B (Liu et al., 2024b)	43.24	42.44	502	37.13	503	38.53	504	35.37	505	35.77	506	37.90	507	39.76
502	MusiLingo-7B (Deng et al., 2024)	43.24	41.93	503	40.12	504	41.23	505	31.23	506	31.73	507	38.10	508	38.29
503	Audio Flamingo-3-8.2B (Goel et al., 2025)	79.58	75.83	504	73.95	505	74.47	506	66.37	507	66.97	508	73.30	72.42	
504	Audio Flamingo-2-3B (Ghosh et al., 2025a)	71.47	68.13	505	70.96	506	70.20	507	44.74	508	44.87	509	62.40	61.06	
505	Audio Flamingo Chat-1B (Kong et al., 2024)	25.3	23.33	506	17.66	507	15.77	508	6.91	509	7.67	510	16.60	15.59	
506	PLITS-MultiEnc-1B (Baseline)	71.17	<b>72.20</b>	507	<b>71.56</b>	508	<b>69.66</b>	509	<b>53.45</b>	510	<b>54.31</b>	511	<b>65.40</b>	512	<b>64.61</b>
507	LAL-MultiEnc-1B (Ours)	71.77	70.39	508	70.96	509	66.50	510	45.65	511	48.17	512	62.80	513	61.85
508	PAL-MultiEnc-1B (Ours)	<b>72.07</b>	70.63	509	70.66	510	66.10	511	<b>53.45</b>	512	53.28	513	<b>65.40</b>	514	63.45
509	PLITS-UniEnc-3B (Baseline)	75.68	72.03	510	<b>70.96</b>	511	69.63	512	46.25	513	46.48	514	64.30	515	62.91
510	PAL-UniEnc-3B(r=3)(Ours)	<b>76.28</b>	<b>73.87</b>	511	69.76	512	<b>70.03</b>	513	<b>49.25</b>	514	<b>54.46</b>	515	<b>65.10</b>	516	<b>66.26</b>

511 Table 6: Evaluation of PAL on **MMAR** (Ma et al., 2025) (accuracy, %). Abbr: Sound (Sn), Music  
 512 (Mu), Speech (Sp) and r (reduction factor, Section 3.3.2). Except for Audio Flamingo 2, all other  
 513 systems use PLITS; their higher scores mainly stem from larger datasets, bigger LLMs, and stronger  
 514 audio encoders. **Boldface** marks PAL multi encoder and unified encoder variants separately, reflect-  
 515 ing our focus on integration.

516	Models	Sn	Mu	Sp	Mix		Mix		Mix	Mix	Total	
					517	Sn-Mu	518	Mix	519	Sd-Sp	520	Accuracy
517	Audio Flamingo-2-3B	24.85	17.48	20.75	18.18	26.61	23.17	8.33	21.90			
518	Audio Flamingo-3-8.2B	-	-	-	-	-	-	-	-	-	-	58.5
519	LTU-7B	19.39	19.90	13.95	18.18	24.77	21.95	16.67	19.20			
520	SALMONN-13B	30.30	31.07	34.69	9.09	34.86	35.37	41.67	33.20			
521	GAMA-7B	29.09	24.27	27.89	27.27	24.77	28.05	20.83	26.50			
522	GAMA-IT-7B	22.42	16.02	12.24	36.36	22.48	14.63	12.50	17.40			
523	Qwen2.5-Omni-7B	58.79	40.78	59.86	54.55	61.93	67.07	58.33	56.70			
524	PLITS-MultiEnc-1B(Baseline)	38.79	<b>42.72</b>	<b>40.48</b>	18.18	44.50	39.02	<b>41.67</b>	41.20			
525	LAL-MultiEnc-1B(Ours)	40.00	40.29	35.71	27.27	42.66	43.90	37.50	39.50			
526	PAL-MultiEnc-1B(Ours)	<b>40.61</b>	41.75	38.10	<b>36.36</b>	<b>45.87</b>	<b>52.44</b>	<b>41.67</b>	<b>42.20</b>			
527	PLITS-UniEnc-3B(Baseline)	38.79	40.29	37.41	<b>36.36</b>	<b>48.17</b>	40.24	<b>50.00</b>	41.10			
528	PAL-UniEnc-3B(r=3)(Ours)	<b>46.61</b>	<b>44.17</b>	<b>40.82</b>	27.27	<b>48.17</b>	<b>46.34</b>	41.67	<b>44.40</b>			

## 5 CONCLUSION

532 We introduce LAL, which injects audio only through attention keys and values and skips feedfor-  
 533 ward processing for audio tokens. This reduces attention interactions and activations, yielding up  
 534 to about 60% lower memory usage and up to about 190% higher training throughput, with per-  
 535 formance comparable to PLITS, the state of the art baseline integration for classification, captioning,  
 536 and reasoning tasks. We also propose PAL, an hybrid integration that uses LAL both PLITS for  
 537 efficient audio-LLM that understand general audio and speech. LAL is a core architectural change  
 538 rather than a parameter efficient fine tuning method, so the efficiency gains hold at inference and  
 539 during training. For future work, we plan to scale to larger backbones, use higher quality instruction  
 540 data to improve reasoning, and explore streaming and long context audio.

540 ETHICS STATEMENT  
541

542 All experiments use publicly available datasets. The proposed approach enables beneficial appli-  
543 cations, but it could also be misused, for example to monitor individuals without consent. We  
544 acknowledge these risks and will release code and models with care, including clear documentation  
545 and use guidance to support responsible research.

546  
547 REPRODUCIBILITY STATEMENT  
548

549 Implementation details are provided in Sections 3.2 and 3.3. Training details appear in Appendix C,  
550 and the evaluation protocol is described in Appendix D. Code and pretrained models will be made  
551 available upon acceptance.

552  
553 REFERENCES  
554

555 Sara Atito Ali Ahmed, Muhammad Awais, Wenwu Wang, Mark D. Plumbley, and Josef Kittler.  
556 Asit: Local-global audio spectrogram vision transformer for event classification. *IEEE/ACM  
557 Transactions on Audio, Speech, and Language Processing*, 32:3684–3693, 2024. ISSN 2329-  
558 9304. doi: 10.1109/taslp.2024.3428908. URL [http://dx.doi.org/10.1109/TASLP.  
559 2024.3428908](http://dx.doi.org/10.1109/TASLP.2024.3428908).

560 Jean-Baptiste Alayrac, Jeff Donahue, Pauline Luc, Antoine Miech, Iain Barr, Yana Hasson, Karel  
561 Lenc, Arthur Mensch, Katherine Millican, Malcolm Reynolds, et al. Flamingo: a visual language  
562 model for few-shot learning. *Advances in neural information processing systems*, 35:23716–  
563 23736, 2022.

564 Tony Alex, Sara Atito, Armin Mustafa, Muhammad Awais, and Philip J B Jackson. SSLAM:  
565 Enhancing self-supervised models with audio mixtures for polyphonic soundscapes. In *The  
566 Thirteenth International Conference on Learning Representations*, 2025. URL <https://openreview.net/forum?id=odU59TxdiB>.

567 Trenton Bricken, Adly Templeton, Joshua Batson, Brian Chen, Adam Jermyn, Tom Con-  
568 erly, Nick Turner, Cem Anil, Carson Denison, Amanda Askell, Robert Lasenby, Yifan Wu,  
569 Shauna Kravec, Nicholas Schiefer, Tim Maxwell, Nicholas Joseph, Zac Hatfield-Dodds, Alex  
570 Tamkin, Karina Nguyen, Brayden McLean, Josiah E Burke, Tristan Hume, Shan Carter,  
571 Tom Henighan, and Christopher Olah. Towards monosematicity: Decomposing language  
572 models with dictionary learning. *Transformer Circuits Thread*, 2023. [https://transformer-  
574 circuits.pub/2023/monosemantic-features/index.html](https://transformer-<br/>573 circuits.pub/2023/monosemantic-features/index.html).

575 Anthony Brohan, Noah Brown, Justice Carbajal, Yevgen Chebotar, Xi Chen, Krzysztof Choroman-  
576 ski, Tianli Ding, Danny Driess, Avinava Dubey, Chelsea Finn, et al. Rt-2: Vision-language-action  
577 models transfer web knowledge to robotic control. *arXiv preprint arXiv:2307.15818*, 2023.

578 Tom Brown, Benjamin Mann, Nick Ryder, Melanie Subbiah, Jared D Kaplan, Prafulla Dhariwal,  
579 Arvind Neelakantan, Pranav Shyam, Girish Sastry, Amanda Askell, et al. Language models are  
580 few-shot learners. *Advances in neural information processing systems*, 33:1877–1901, 2020.

581 Carlos Busso, Murtaza Bulut, Chi-Chun Lee, Abe Kazemzadeh, Emily Mower, Samuel Kim, Jean-  
582 nette N Chang, Sungbok Lee, and Shrikanth S Narayanan. Iemocap: Interactive emotional dyadic  
583 motion capture database. *Language resources and evaluation*, 42(4):335–359, 2008.

584 Wenxi Chen, Yuzhe Liang, Ziyang Ma, Zhisheng Zheng, and Xie Chen. Eat: Self-supervised pre-  
585 training with efficient audio transformer. *arXiv preprint arXiv:2401.03497*, 2024.

586 Yunfei Chu, Jin Xu, Xiaohuan Zhou, Qian Yang, Shiliang Zhang, Zhijie Yan, Chang Zhou, and  
587 Jingren Zhou. Qwen-audio: Advancing universal audio understanding via unified large-scale  
588 audio-language models, 2023. URL <https://arxiv.org/abs/2311.07919>.

589 Yunfei Chu, Jin Xu, Qian Yang, Haojie Wei, Xipin Wei, Zhifang Guo, Yichong Leng, Yuanjun Lv,  
590 Jinzheng He, Junyang Lin, Chang Zhou, and Jingren Zhou. Qwen2-audio technical report, 2024.  
591 URL <https://arxiv.org/abs/2407.10759>.

594 Zihao Deng, Yinghao Ma, Yudong Liu, Rongchen Guo, Ge Zhang, Wenhua Chen, Wenhao Huang,  
 595 and Emmanouil Benetos. Musilingo: Bridging music and text with pre-trained language models  
 596 for music captioning and query response, 2024. URL <https://arxiv.org/abs/2309.08730>.

598 Soham Deshmukh, Benjamin Elizalde, Rita Singh, and Huaming Wang. Pensi: An audio language  
 599 model for audio tasks. *Advances in Neural Information Processing Systems*, 36, 2023.

600 Soham Deshmukh, Shuo Han, Hazim Bukhari, Benjamin Elizalde, Hannes Gamper, Rita Singh,  
 601 and Bhiksha Raj. Audio entailment: Assessing deductive reasoning for audio understanding.  
 602 In *Proceedings of the AAAI Conference on Artificial Intelligence*, volume 39, pp. 23769–23777,  
 603 2025a.

604 Soham Deshmukh, Shuo Han, Rita Singh, and Bhiksha Raj. Adiff: Explaining audio difference  
 605 using natural language. *arXiv preprint arXiv:2502.04476*, 2025b.

606 Konstantinos Drossos, Samuel Lipping, and Tuomas Virtanen. Clotho: An audio captioning dataset.  
 607 In *ICASSP 2020-2020 IEEE International Conference on Acoustics, Speech and Signal Processing (ICASSP)*, pp. 736–740. IEEE, 2020.

608 Nelson Elhage, Tristan Hume, Catherine Olsson, Nicholas Schiefer, Tom Henighan, Shauna Kravec,  
 609 Zac Hatfield-Dodds, Robert Lasenby, Dawn Drain, Carol Chen, Roger Grosse, Sam McCandlish,  
 610 Jared Kaplan, Dario Amodei, Martin Wattenberg, and Christopher Olah. Toy models of super-  
 611 position. *Transformer Circuits Thread*, 2022. [https://transformer-circuits.pub/2022/toy\\_model/index.html](https://transformer-circuits.pub/2022/toy_model/index.html).

612 Benjamin Elizalde, Soham Deshmukh, Mahmoud Al Ismail, and Huaming Wang. Clap learning  
 613 audio concepts from natural language supervision. In *ICASSP 2023-2023 IEEE International  
 614 Conference on Acoustics, Speech and Signal Processing (ICASSP)*, pp. 1–5. IEEE, 2023.

615 Eduardo Fonseca, Xavier Favory, Jordi Pons, Frederic Font, and Xavier Serra. Fsd50k: an open  
 616 dataset of human-labeled sound events. *IEEE/ACM Transactions on Audio, Speech, and Language  
 617 Processing*, 30:829–852, 2021.

618 Jort F Gemmeke, Daniel PW Ellis, Dylan Freedman, Aren Jansen, Wade Lawrence, R Channing  
 619 Moore, Manoj Plakal, and Marvin Ritter. Audio set: An ontology and human-labeled dataset for  
 620 audio events. In *2017 IEEE international conference on acoustics, speech and signal processing  
 621 (ICASSP)*, pp. 776–780. IEEE, 2017.

622 Sreyan Ghosh, Sonal Kumar, Ashish Seth, Chandra Kiran Reddy Evuru, Utkarsh Tyagi, S Sakshi,  
 623 Oriol Nieto, Ramani Duraiswami, and Dinesh Manocha. Gama: A large audio-language  
 624 model with advanced audio understanding and complex reasoning abilities. *arXiv preprint  
 625 arXiv:2406.11768*, 2024.

626 Sreyan Ghosh, Zhifeng Kong, Sonal Kumar, S Sakshi, Jaehyeon Kim, Wei Ping, Rafael Valle, Dinesh  
 627 Manocha, and Bryan Catanzaro. Audio flamingo 2: An audio-language model with long-  
 628 audio understanding and expert reasoning abilities. *arXiv preprint arXiv:2503.03983*, 2025a.

629 Sreyan Ghosh, Sonal Kumar, Chandra Kiran Reddy Evuru, Oriol Nieto, Ramani Duraiswami, and  
 630 Dinesh Manocha. Reclap: Improving zero shot audio classification by describing sounds. In  
 631 *ICASSP 2025-2025 IEEE International Conference on Acoustics, Speech and Signal Processing  
 632 (ICASSP)*, pp. 1–5. IEEE, 2025b.

633 Arushi Goel, Sreyan Ghosh, Jaehyeon Kim, Sonal Kumar, Zhifeng Kong, Sang-gil Lee, Chao-  
 634 Han Huck Yang, Ramani Duraiswami, Dinesh Manocha, Rafael Valle, et al. Audio flamingo  
 635 3: Advancing audio intelligence with fully open large audio language models. *arXiv preprint  
 636 arXiv:2507.08128*, 2025.

637 Yuan Gong, Yu-An Chung, and James Glass. Ast: Audio spectrogram transformer. *arXiv preprint  
 638 arXiv:2104.01778*, 2021.

639 Yuan Gong, Andrew Rouditchenko, Alexander H Liu, David Harwath, Leonid Karlinsky, Hilde  
 640 Kuehne, and James Glass. Contrastive audio-visual masked autoencoder. *arXiv preprint  
 641 arXiv:2210.07839*, 2022a.

648 Yuan Gong, Jin Yu, and James Glass. Vocalsound: A dataset for improving human vocal sounds  
 649 recognition. In *ICASSP 2022-2022 IEEE International Conference on Acoustics, Speech and*  
 650 *Signal Processing (ICASSP)*, pp. 151–155. IEEE, 2022b.

651

652 Yuan Gong, Sameer Khurana, Leonid Karlinsky, and James Glass. Whisper-at: Noise-robust  
 653 automatic speech recognizers are also strong general audio event taggers. *arXiv preprint*  
 654 *arXiv:2307.03183*, 2023a.

655 Yuan Gong, Alexander H Liu, Hongyin Luo, Leonid Karlinsky, and James Glass. Joint audio and  
 656 speech understanding. In *2023 IEEE Automatic Speech Recognition and Understanding Work-*  
 657 *shop (ASRU)*, pp. 1–8. IEEE, 2023b.

658 Yuan Gong, Hongyin Luo, Alexander H. Liu, Leonid Karlinsky, and James R. Glass. Listen, think,  
 659 and understand. In *The Twelfth International Conference on Learning Representations*, 2024.  
 660 URL <https://openreview.net/forum?id=nBZBPXdJ1C>.

661

662 Aaron Grattafiori, Abhimanyu Dubey, Abhinav Jauhri, Abhinav Pandey, Abhishek Kadian, Ahmad  
 663 Al-Dahle, Aiesha Letman, Akhil Mathur, Alan Schelten, Alex Vaughan, et al. The llama 3 herd  
 664 of models. *arXiv preprint arXiv:2407.21783*, 2024.

665 Khaled Hechmi, Trung Ngo Trong, Ville Hautamäki, and Tomi Kinnunen. Voxceleb enrichment  
 666 for age and gender recognition. In *2021 IEEE Automatic Speech Recognition and Understanding*  
 667 *Workshop (ASRU)*, pp. 687–693. IEEE, 2021.

668

669 Edward J Hu, Yelong Shen, Phillip Wallis, Zeyuan Allen-Zhu, Yuanzhi Li, Shean Wang, Lu Wang,  
 670 Weizhu Chen, et al. Lora: Low-rank adaptation of large language models. *ICLR*, 1(2):3, 2022.

671 Po-Yao Huang, Hu Xu, Juncheng Li, Alexei Baevski, et al. Masked autoencoders that listen. In  
 672 *Proc. NeurIPS*, 2022.

673

674 Albert Q Jiang, Alexandre Sablayrolles, Antoine Roux, Arthur Mensch, Blanche Savary, Chris Bam-  
 675 ford, Devendra Singh Chaplot, Diego de las Casas, Emma Bou Hanna, Florian Bressand, et al.  
 676 Mixtral of experts. *arXiv preprint arXiv:2401.04088*, 2024.

677 Chris Dongjoo Kim, Byeongchang Kim, Hyunmin Lee, and Gunhee Kim. Audiocaps: Generating  
 678 captions for audios in the wild. In *Proceedings of the 2019 Conference of the North American*  
 679 *Chapter of the Association for Computational Linguistics: Human Language Technologies, Vol-*  
 680 *ume 1 (Long and Short Papers)*, pp. 119–132, 2019.

681

682 Zhifeng Kong, Arushi Goel, Rohan Badlani, Wei Ping, Rafael Valle, and Bryan Catanzaro. Audio  
 683 flamingo: A novel audio language model with few-shot learning and dialogue abilities. In *Forty-*  
 684 *first International Conference on Machine Learning*, 2024. URL <https://openreview.net/forum?id=WYi3WKZjYe>.

685

686 Junnan Li, Dongxu Li, Silvio Savarese, and Steven Hoi. Blip-2: Bootstrapping language-image  
 687 pre-training with frozen image encoders and large language models. In *International conference*  
 688 *on machine learning*, pp. 19730–19742. PMLR, 2023.

689

690 Aixin Liu, Bei Feng, Bing Xue, Bingxuan Wang, Bochao Wu, Chengda Lu, Chenggang Zhao,  
 691 Chengqi Deng, Chenyu Zhang, Chong Ruan, et al. Deepseek-v3 technical report. *arXiv preprint*  
 692 *arXiv:2412.19437*, 2024a.

693

694 Haotian Liu, Chunyuan Li, Qingyang Wu, and Yong Jae Lee. Visual instruction tuning. *Advances*  
 695 *in neural information processing systems*, 36:34892–34916, 2023.

696

697 Shansong Liu, Atin Sakkeer Hussain, Qilong Wu, Chenshuo Sun, and Ying Shan. M<sup>2</sup>ugen: Multi-  
 698 modal music understanding and generation with the power of large language models, 2024b. URL  
 699 <https://arxiv.org/abs/2311.11255>.

700

701 Ilya Loshchilov and Frank Hutter. SGDR: Stochastic gradient descent with warm restarts. *arXiv*  
 702 *preprint arXiv:1608.03983*, 2016.

703

704 Ilya Loshchilov and Frank Hutter. Decoupled weight decay regularization. *arXiv preprint*  
 705 *arXiv:1711.05101*, 2017.

702 Ke-Han Lu, Zhehuai Chen, Szu-Wei Fu, Chao-Han Huck Yang, Sung-Feng Huang, Chih-Kai Yang,  
 703 Chee-En Yu, Chun-Wei Chen, Wei-Chih Chen, Chien Yu Huang, Yi-Cheng Lin, Yu-Xiang Lin,  
 704 Chi-An Fu, Chun-Yi Kuan, Wenze Ren, Xuanjun Chen, Wei-Ping Huang, En-Pei Hu, Tzu-Quan  
 705 Lin, Yuan-Kuei Wu, Kuan-Po Huang, Hsiao-Ying Huang, Huang-Cheng Chou, Kai-Wei Chang,  
 706 Cheng-Han Chiang, Boris Ginsburg, Yu-Chiang Frank Wang, and Hung yi Lee. Desta2.5-audio:  
 707 Toward general-purpose large audio language model with self-generated cross-modal alignment,  
 708 2025. URL <https://arxiv.org/abs/2507.02768>.

709 Ziyang Ma, Yinghao Ma, Yanqiao Zhu, Chen Yang, Yi-Wen Chao, Ruiyang Xu, Wenxi Chen,  
 710 Yuanzhe Chen, Zhuo Chen, Jian Cong, et al. Mmar: A challenging benchmark for deep rea-  
 711 soning in speech, audio, music, and their mix. *arXiv preprint arXiv:2505.13032*, 2025.

712

713 A. Mesaros, A. Diment, B. Elizalde, T. Heittola, E. Vincent, B. Raj, and T. Virtanen. Sound event de-  
 714 tection in the DCASE 2017 challenge. *IEEE/ACM Transactions on Audio, Speech, and Language*  
 715 *Processing*, 2019. ISSN 2329-9290. doi: 10.1109/TASLP.2019.2907016. In press.

716

717 Karol J Piczak. Esc: Dataset for environmental sound classification. In *Proceedings of the 23rd*  
 718 *ACM international conference on Multimedia*, pp. 1015–1018, 2015.

719

720 Alec Radford, Jong Wook Kim, Tao Xu, Greg Brockman, Christine McLeavey, and Ilya Sutskever.  
 721 Robust speech recognition via large-scale weak supervision. In *International conference on ma-*  
 722 *chine learning*, pp. 28492–28518. PMLR, 2023.

723

724 S Sakshi, Utkarsh Tyagi, Sonal Kumar, Ashish Seth, Ramaseswaran Selvakumar, Oriol Nieto, Ra-  
 725 mani Duraiswami, Sreyan Ghosh, and Dinesh Manocha. Mmau: A massive multi-task audio  
 726 understanding and reasoning benchmark. *arXiv preprint arXiv:2410.19168*, 2024.

727

728 Changli Tang, Wenyi Yu, Guangzhi Sun, Xianzhao Chen, Tian Tan, Wei Li, Lu Lu, Zejun MA,  
 729 and Chao Zhang. SALMONN: Towards generic hearing abilities for large language models.  
 730 In *The Twelfth International Conference on Learning Representations*, 2024. URL <https://openreview.net/forum?id=14rn7HpKVk>.

731

732 Qwen Team. Qwen2.5: A party of foundation models, September 2024. URL <https://qwenlm.github.io/blog/qwen2.5/>.

733

734 Adly Templeton, Tom Conerly, Jonathan Marcus, Jack Lindsey, Trenton Bricken, Brian Chen,  
 735 Adam Pearce, Craig Citro, Emmanuel Ameisen, Andy Jones, Hoagy Cunningham, Nicholas L  
 736 Turner, Callum McDougall, Monte MacDiarmid, C. Daniel Freeman, Theodore R. Sumers,  
 737 Edward Rees, Joshua Batson, Adam Jermyn, Shan Carter, Chris Olah, and Tom Henighan.  
 738 Scaling monosemanticity: Extracting interpretable features from claude 3 sonnet. *Trans-*  
 739 *former Circuits Thread*, 2024. URL <https://transformer-circuits.pub/2024/scaling-monosemanticity/index.html>.

740

741 Omkar Thawkar, Abdelrahman Shaker, Sahal Shaji Mullappilly, Hisham Cholakkal, Rao Muham-  
 742 mad Anwer, Salman Khan, Jorma Laaksonen, and Fahad Shahbaz Khan. Xraygpt: Chest radio-  
 743 graphs summarization using medical vision-language models. *arXiv preprint arXiv:2306.07971*,  
 744 2023.

745

746 Peter Tong, Ellis Brown, Penghao Wu, Sanghyun Woo, Adithya Jairam Vedagiri IYER, Sai Charitha  
 747 Akula, Shusheng Yang, Jihan Yang, Manoj Middepogu, Ziteng Wang, et al. Cambrian-1: A fully  
 748 open, vision-centric exploration of multimodal llms. *Advances in Neural Information Processing*  
 749 *Systems*, 37:87310–87356, 2024.

750

751 Dingdong Wang, Jincenzi Wu, Junan Li, Dongchao Yang, Xueyuan Chen, Tianhua Zhang, and  
 752 Helen Meng. Mmsu: A massive multi-task spoken language understanding and reasoning bench-  
 753 mark. *arXiv preprint arXiv:2506.04779*, 2025.

754

755 Weihang Wang, Qingsong Lv, Wenmeng Yu, Wenyi Hong, Ji Qi, Yan Wang, Junhui Ji, Zhuoyi Yang,  
 756 Lei Zhao, Song XiXuan, et al. Cogvilm: Visual expert for pretrained language models. *Advances*  
 757 *in Neural Information Processing Systems*, 37:121475–121499, 2024.

756 Boyong Wu, Chao Yan, Chen Hu, Cheng Yi, Chengli Feng, Fei Tian, Feiyu Shen, Gang Yu, Haoyang  
 757 Zhang, Jingbei Li, Mingrui Chen, Peng Liu, Wang You, Xiangyu Tony Zhang, Xingyuan Li,  
 758 Xuerui Yang, Yayue Deng, Yechang Huang, Yuxin Li, Yuxin Zhang, Zhao You, Brian Li, Changyi  
 759 Wan, Hanpeng Hu, Jiangjie Zhen, Siyu Chen, Song Yuan, Xuelin Zhang, Yimin Jiang, Yu Zhou,  
 760 Yuxiang Yang, Bingxin Li, Buyun Ma, Changhe Song, Dongqing Pang, Guoqiang Hu, Haiyang  
 761 Sun, Kang An, Na Wang, Shuli Gao, Wei Ji, Wen Li, Wen Sun, Xuan Wen, Yong Ren, Yuankai  
 762 Ma, Yufan Lu, Bin Wang, Bo Li, Changxin Miao, Che Liu, Chen Xu, Dapeng Shi, Dingyuan  
 763 Hu, Donghang Wu, Enle Liu, Guanzhe Huang, Gulin Yan, Han Zhang, Hao Nie, Haonan Jia,  
 764 Hongyu Zhou, Jianjian Sun, Jiaoren Wu, Jie Wu, Jie Yang, Jin Yang, Junzhe Lin, Kaixiang Li, Lei  
 765 Yang, Liying Shi, Li Zhou, Longlong Gu, Ming Li, Mingliang Li, Mingxiao Li, Nan Wu, Qi Han,  
 766 Qinyuan Tan, Shaoliang Pang, Shengjie Fan, Siqi Liu, Tiancheng Cao, Wanying Lu, Wenqing He,  
 767 Wuxun Xie, Xu Zhao, Xueqi Li, Yanbo Yu, Yang Yang, Yi Liu, Yifan Lu, Yilei Wang, Yuanhao  
 768 Ding, Yuanwei Liang, Yuanwei Lu, Yuchu Luo, Yuhe Yin, Yumeng Zhan, Yuxiang Zhang, Zidong  
 769 Yang, Zixin Zhang, Binxing Jiao, Dixin Jiang, Heung-Yeung Shum, Jiansheng Chen, Jing Li,  
 770 Xiangyu Zhang, and Yibo Zhu. Step-audio 2 technical report, 2025a. URL <https://arxiv.org/abs/2507.16632>.  
 771

772 Boyong Wu, Chao Yan, Chen Hu, Cheng Yi, Chengli Feng, Fei Tian, Feiyu Shen, Gang Yu, Haoyang  
 773 Zhang, Jingbei Li, et al. Step-audio 2 technical report. *arXiv preprint arXiv:2507.16632*, 2025b.

774  
 775 Yusong Wu, Ke Chen, Tianyu Zhang, Yuchen Hui, Taylor Berg-Kirkpatrick, and Shlomo Dubnov.  
 776 Large-scale contrastive language-audio pretraining with feature fusion and keyword-to-caption  
 777 augmentation. In *ICASSP 2023-2023 IEEE International Conference on Acoustics, Speech and  
 778 Signal Processing (ICASSP)*, pp. 1–5. IEEE, 2023.

779  
 780 Jin Xu, Zhifang Guo, Jinzheng He, Hangrui Hu, Ting He, Shuai Bai, Keqin Chen, Jialin Wang, Yang  
 781 Fan, Kai Dang, Bin Zhang, Xiong Wang, Yunfei Chu, and Junyang Lin. Qwen2.5-omni technical  
 782 report, 2025. URL <https://arxiv.org/abs/2503.20215>.

## 783 784 A APPENDIX

## 785 B LLM USAGE

786 Large language models were used only as assistive tools for editing and polishing text. We followed  
 787 the benchmark protocol of Ghosh et al. (2024) to rate audio LLM outputs; the GPT based evaluation  
 788 is part of that benchmark. See Section 4.1 for details. LLMs were not used for model design, data  
 789 selection, experiment setup, implementation, analysis, or generation of results. All technical content  
 790 was written and verified by the authors.

## 791 C TRAINING DETAILS

### 792 C.1 LAL TRAINING DETAILS

793 We use OpenAQA (Gong et al., 2024) two stage training setup for LAL to report the results in  
 794 Table 1. We also train on broader open ended data from OpenAQA (Gong et al., 2024) and on the  
 795 reasoning dataset CompA R (Ghosh et al., 2024), with evaluations shown in Table 2. Additional  
 796 training hyperparameters appear in Table 7.

### 801 C.2 PAL TRAINING DETAILS

802 PAL uses a two stage training protocol(Table 8). In Stage 1, we start from the Stage 1 dataset  
 803 used for LAL and augment it with additional speech focused data from OpenASQA (Gong et al.,  
 804 2023b). In Stage 2, we fine tune on a curated audio, speech, and music reasoning instruction corpus,  
 805 AudioSkills (Goel et al., 2025). We use a 6M example subset of AudioSkills (from the original  
 806 10M) due to the unavailability of original audio files for some source datasets.

810

811

Table 7: Hyper-parameters used for the three stage training of **LAL** and **PLITS** (Llama3.2 1B)

Training Configuration	Stage 1 (Connector Pre training)	Stage 2 (LLM Fine tuning)	Stage 3   Stage 4 (LLM Fine tuning)
Optimizer		AdamW (Loshchilov & Hutter, 2017)	
Learning Rate Schedule		Cosine (Loshchilov & Hutter, 2016)	
Peak Learning Rate	0.001	0.0001	0.0001
Epochs	1	1	1
Warm up Ratio (steps)	0.05	0.03	0.03
Dataset Size	1.2 M	1.9 M	5.6 M   200 K
Batch Size	32	12	12
Gradient Accumulation Steps		4	
GPUs		2 × Nvidia A100 (80GB)	
RAM		150 GB	
Loss		Next token loss on text part	

823

824

Table 8: Hyperparameters used for the two stage training of **PAL** and **PLITS** (Llama3.2 1B)

Training Configuration	Stage 1 (Connector Pre training)	Stage 2 (LLM Fine tuning)
Optimizer	AdamW (Loshchilov & Hutter, 2017)	
Learning Rate Schedule	Cosine (Loshchilov & Hutter, 2016)	
Peak Learning Rate	0.001	0.0001
Epochs	1	1
Warm up Ratio (steps)	0.05	0.03
Dataset Size	1.7 M	6.4 M
Batch Size	16	4
Gradient Accumulation Steps	2	32
GPUs	4 × Nvidia A100 (64GB)	
RAM	250 GB	
Loss	Next token loss on text part	

837

838

## D EVALUATION DETAILS

841

### D.1 LAL EVALUATION DETAILS

843

We follow the evaluation protocol of Gong et al. (2024) for classification and captioning, and use the CompA R test set of Ghosh et al. (2024) for reasoning. Below we summarize the datasets included in the Gong et al. (2024) protocol.

847

**VocalSound** (Gong et al., 2022b): The VocalSound dataset consists of 21,024 crowd-sourced recordings of 6 different classes of vocal expressions collected from 3,365 unique subjects. We evaluated our model on the VocalSound evaluation set which contains 3,594 audio clips, and report top-1 accuracy scores across the 6 classes for single-class classification performance. It is important to note that VocalSound was excluded from our training data; therefore, our evaluation on VocalSound is considered zero-shot.

853

**ESC-50** (Piczak, 2015): The ESC-50 dataset comprises 2,000 five-second environmental audio clips categorized into 50 different classes. Following Gong et al. (2024), we evaluate our model on all 2,000 audio samples and report the top-1 accuracy score for single-class classification performance. It is important to note that while ESC-50 is originally sampled from the Freesound dataset (which is included in our training data), ESC-50 itself was excluded from training. Therefore, our evaluation on this dataset is considered a weak zero-shot evaluation.

859

860

861

862

863

**DCASE2017 task 4** (DCASE) (Mesaros et al., 2019): DCASE 2017 Task 4 contains 17 sound events distributed across two categories: "Warning" and "Vehicle". The evaluation set consists of 1,350 audio clips. We evaluated our model on this dataset and report micro F1-score(MiF1) for single-class classification performance. It is important to note that DCASE 2017 task 4 is originally sampled from AudioSet, which is included in our training data. However, DCASE 2017 task 4 itself is excluded from training, making our evaluation on this dataset a weak zero-shot evaluation.

**FSD50K** (FSD) (Fonseca et al., 2021): The FSD50K evaluation set contains 10,231 audio clips. We evaluated our model on this evaluation set and report the mAP score for multi-label classification performance. Since the training and validation sets of FSD50K are included in our training data, this evaluation is considered an in-domain evaluation.

**AudioSet** (Gemmeke et al., 2017): We evaluated our model on this evaluation set and report the mAP score for multi-label classification performance. The training set of AudioSet is included in our training data, making this evaluation an in-domain evaluation.

**AudioCaps** (Kim et al., 2019): The AudioCaps evaluation set contains 901 audio clips, each paired with 5 audio captions, resulting in a total of 4,505 audio-caption pairs. We evaluated our model on this evaluation set and report the captioning scores using CIDEr and SPICE metrics. The training and validation sets of AudioCaps are included in our training data, making this evaluation an in-domain evaluation.

**Clotho V2** (Drossos et al., 2020): The Clotho V2 evaluation set contains 1,045 audio clips, each paired with 5 audio captions, resulting in a total of 5,225 audio-caption pairs. We evaluated our model on this evaluation set and report the captioning scores using CIDEr and SPICE metrics. The development and validation sets of Clotho V2 are included in our training data, making this evaluation an in-domain evaluation.

## D.2 PAL EVALUATION DETAILS

For speech classification (emotion recognition and gender classification), we follow the protocol of Gong et al. (2023b). For combined sound, speech, and music reasoning, we evaluate on the standard benchmark datasets MMAU (Sakshi et al., 2024) and MMAR (Ma et al., 2025).

## E LAL INTEGRATION WITH FROZEN LLM FFN

Standard audio-LLM training typically requires full fine tuning of the LLM. However, since LAL integrates audio information solely through the attention mechanism, we investigate whether LAL remains effective when the LLM feedforward (FFN) blocks, which are widely believed to encode much of the model’s factual and linguistic knowledge, are frozen and only the attention layers are updated. In Stage 2 of our training pipeline, we therefore construct a variant with the LLM FFN frozen. As shown in Table 9, performance is largely maintained under this setting. This result suggests that LAL can successfully integrate audio information through attention without modifying the knowledge stored in the FFN modules. Such a property has important implications for reducing training cost, improving parameter efficiency, and preserving the pretrained knowledge of the LLM while enabling multimodal alignment.

Table 9: Performance evaluation of the **LAL** Integration with frozen FFN. Evaluation follows the protocol of Gong et al. (2024). AC: Audio caps, CL:Clotho AS2M: AudioSet 2M <sup>†</sup> indicates CIDEr and <sup>‡</sup> indicates SPICE. Metrics: accuracy (ESC-50, VocalSound), Mi-F1 (DCASE), and mAP (FSD, AudioSet). Complete evaluation methodology explained in Section 4.1 and dataset details in Appendix D

907 908 909 910 911 912 913 914 915 916 917	LLM Backbone	FFN Frozen	PLITS	LAL	LFST	Classification						Captioning		
						ESC50	DCASE	VS	FSD	AS2M	AC <sup>†</sup>	CL <sup>†</sup>	AC <sup>‡</sup>	CL <sup>‡</sup>
	Llama3.2-1B	✗	✓	✗	✗	64.45	37.69	51.57	25.23	9.08	0.59	0.34	16.30	10.96
		✗	✗	✓	✗	<b>76.70</b>	<b>40.97</b>	<b>60.87</b>	<b>31.44</b>	<b>11.83</b>	<b>0.66</b>	0.38	<b>16.97</b>	<b>11.87</b>
		✓	✗	✓	✗	71.80	33.99	55.28	29.38	10.48	0.63	<b>0.40</b>	16.11	11.75

## E.1 LFST CONNECTOR: LANGUAGE ALIGNED AND FINE GRAINED SPATIOTEMPORAL CONNECTOR

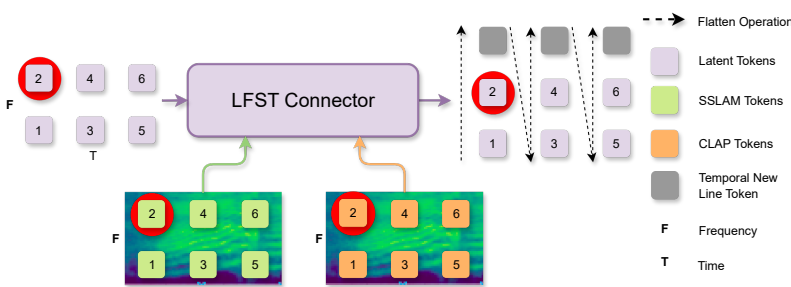
We adopt the connector *proposed in Cambrian* (Tong et al., 2024) and apply it in our audio setting to fuse a language aligned encoder such as CLAP with a self supervised encoder such as SSLAM. The connector produces a compact set of latent tokens that combine semantic cues from CLAP with

918 fine grained spatiotemporal detail from SSLAM, while keeping sequence length fixed and avoiding  
 919 the overhead of naive concatenation.  
 920

921 **Formalization.** Let the encoder outputs be  
 922

$$H_{\text{sslam}}, H_{\text{clap}} \in \mathbb{R}^{F \times T \times d}, \quad z \in \mathbb{R}^d,$$

924 where  $F$  is frequency,  $T$  is time, and  $d$  is the feature dimension. Following Tong et al. (2024),  
 925 a single latent token  $z$  is broadcast to each spatiotemporal location, yielding  $z_{f,t}$  for every  $(f, t)$ .  
 926 Inside the connector, which consists of 3 cross attention layers, each  $z_{f,t}$  is updated through cross  
 927 attention with the corresponding local regions of  $H_{\text{sslam}}$  and  $H_{\text{clap}}$ . To preserve temporal structure  
 928 when flattening across  $(F, T)$ , we insert a *newline token* along the frequency axis so that each new  
 929 time step begins with this marker before its spectral tokens (see Figure 3).  
 930



921 Figure 3: Overview of LFST using the Cambrian connector (Tong et al., 2024). A single latent  
 922 token is broadcast to every time–frequency location and then updated inside the connector by cross  
 923 attention with local SSLAM and CLAP features, fusing fine grained spatiotemporal detail with  
 924 language aligned semantics. The red tokens illustrate the latent query and the local encoder keys  
 925 and values it attends to. A newline token is inserted at each new time step so the flattened sequence  
 926 preserves the original spatiotemporal layout while keeping the output length fixed.  
 927

## 928 E.2 PAL 2 VARIANTS: MULTI AUDIO ENCODER AND UNIFIED AUDIO ENCODER 929 VISUALIZATIONS

930 This section provides visualizations of the two PAL variants discussed in Section 3.3.1 and Section  
 931 3.3.2. The multi-encoder audio configuration is illustrated in Figure 4, while the unified audio  
 932 encoder configuration is presented in Figure 5.  
 933

934 Table 10: Performance metrics for PLITS and PAL unified encoder variants. Throughput (Samples/s) and memory (VRAM) are measured during training and inference. Evaluation metrics (MMAR, MMAU, MMSU) represent average performance across benchmark tasks. r (reduction factor, Section 3.3.2). ( $\uparrow$  = higher is better,  $\downarrow$  = lower is better).  
 935

936 Model	937 Training/Inference			938 Evaluation Performance		
	939 Samples/s $\uparrow$	940 VRAM (GB) $\downarrow$	941 MMAR $\uparrow$	942 MMAU $\uparrow$	943 MMSU $\uparrow$	944
945 PLITS-UniEnc-3B	946 70.68/7.80	947 42.49/17.68	948 41.10	949 62.91	950 40.12	951
952 PAL-UniEnc-3B(r=3)	953 96.12/8.40	954 41.48/12.99	955 <b>44.40</b>	956 <b>66.26</b>	957 <b>43.44</b>	958
959 PAL-UniEnc-3B(r=5)	960 <b>105.72/8.76</b>	961 <b>39.98/11.71</b>	962 42.00	963 63.42	964 41.22	965

## 966 E.3 LAL vs. PLITS INTEGRATION FOR SPEECH

967 In this section, we provide a detailed analysis of different integration strategies for the speech modality.  
 968 While LAL demonstrates high efficiency and strong performance for general audio events, our  
 969 experiments indicate that speech understanding, which requires decoding linguistic content, benefits  
 970 significantly from the PLITS integration strategy. This observation motivates our hybrid PAL  
 971 architecture.  
 972

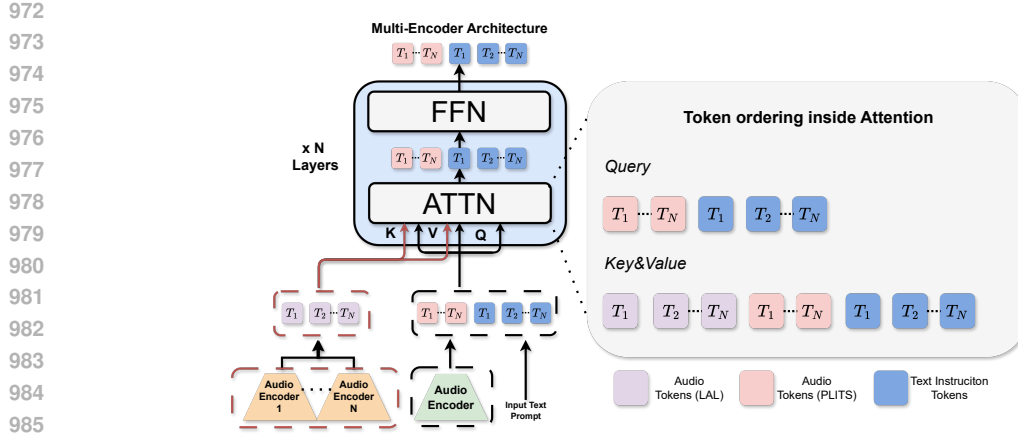


Figure 4: Overview of Multi-Encoder Architecture. Multiple audio encoders process input audio in parallel, with each encoder producing audio tokens. Purple tokens in the diagram represent audio tokens that follow LAL integration  $[T_1^{LAL}, \dots, T_N^{LAL}]$ , while red tokens represent audio tokens that follow PLITS integration  $[T_1^{PLITS}, \dots, T_N^{PLITS}]$ . Blue tokens represent text instruction tokens  $[T_1^{text}, \dots, T_N^{text}]$ . In the attention mechanism, the query is ordered as  $[T^{PLITS}, T^{text}]$ . The key and value tensors are ordered as  $[T^{LAL}, T^{PLITS}, T^{text}]$ .

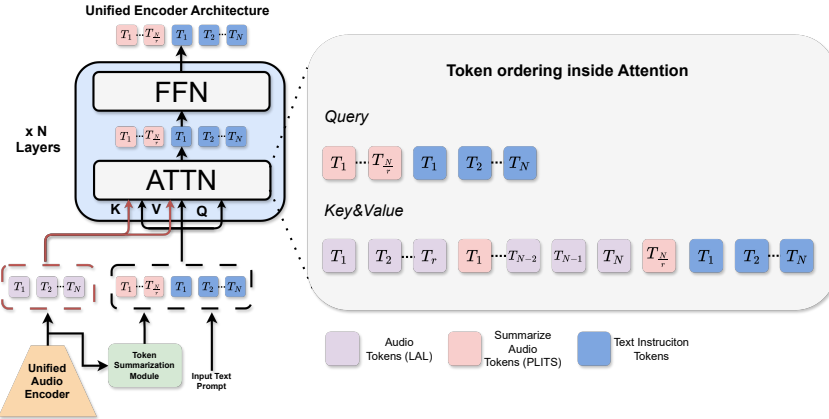


Figure 5: Overview of PAL integration with unified audio encoder. The unified audio encoder processes input audio and produces audio tokens that are split into two paths. Tokens following LAL integration are  $[T_1^{LAL}, \dots, T_N^{LAL}]$ , while token summarization reduces them by factor  $r$  for PLITS integration producing  $[T_1^{PLITS}, \dots, T_{N/r}^{PLITS}]$ . Purple tokens represent LAL audio tokens, red tokens represent summarized PLITS audio tokens, and blue tokens represent text tokens  $[T_1^{text}, \dots, T_N^{text}]$ . In the attention mechanism, the query is ordered as  $[T^{PLITS}, T^{text}]$  from PLITS integration, while the key and value tensors are ordered as the interleaving of audio tokens  $T^{LAL}$  with their corresponding summarized tokens  $T^{PLITS}$ , then text tokens  $T^{text}$  (Section 3.3.2).

**Speech Classification (IEMOCAP & VoxCeleb2).** We evaluate on speech-specific classification tasks: emotion recognition (IEMOCAP) and gender classification (VoxCeleb2). Table 11 compares three configurations: pure PLITS (both encoders use PLITS), pure LAL (both use LAL), and the hybrid PAL configuration (general audio via LAL, speech via PLITS). While the pure LAL configuration performs comparably to pure PLITS on these classification tasks, the hybrid PAL configuration yields the highest accuracy on both datasets (68.81% on IEMOCAP and 97.99% on VoxCeleb2).

1026  
 1027 **Speech Understanding and Reasoning (MMSU).** Further evaluation on speech understanding we  
 1028 benchmark using the MMSU: A Massive Multi-task Spoken Language Understanding and Reasoning  
 1029 Benchmark(MMSU) (Wang et al., 2025). Table 12 presents the performance of Multi-Encoder  
 1030 models on the MMSU, which assesses both paralinguistic and linguistic capabilities. We observe a  
 1031 clear performance gap between the pure PLITS and pure LAL baselines: the LAL-MultiEnc model  
 1032 under performs the PLITS-MultiEnc baseline. The PAL architecture, which routes speech through  
 1033 PLITS and general audio through LAL, recovers this performance loss.

1034 These results substantiate our architectural choice for PAL: treating speech as a “language-like”  
 1035 modality that requires deeper integration via PLITS, while treating general audio as “contextual”  
 1036 information that is well suited for the lightweight LAL integration.

1037  
 1038 **Table 11:** Integration choices for Whisper and CLAP/SSALM on multiple audio encoder setting  
 1039 (Section 3.3.1) evaluated on IEMOCAP (Busso et al., 2008) (emotion recog.) and Vox-  
 1040 Celeb2 (Hechmi et al., 2021) (gender cls.) (accuracy, %).

SSLAM+CLAP Integration	Whisper Integration	IEMOCAP	Voxceleb2
PLITS	PLITS	65.67	96.69
LAL	LAL	66.88	97.19
LAL	PLITS	<b>68.81</b>	<b>97.99</b>

1041  
 1042  
 1043  
 1044  
 1045  
 1046 **Table 12: Evaluation of PLITS, LAL, and PAL on MMSU (accuracy).** Abbr: P-Per = Paralinguistic  
 1047 Perception, L-Per = Linguistic Perception, L-Res = Linguistic Reasoning, P-Res = Paralinguistic  
 1048 Reasoning, Per = Perception (avg), Res = Reasoning (avg), r (reduction factor, Section 3.3.2)

Model	MMSU						
	P-Per	L-Per	L-Res	P-Res	Per	Res	Overall
PLITS-MultiEnc-1B	<b>33.86</b>	<b>33.69</b>	58.47	45.67	<b>33.76</b>	56.69	<b>44.86</b>
LAL-MultiEnc-1B	33.56	30.32	51.08	<b>46.27</b>	31.59	50.41	40.70
PAL-MultiEnc-1B	32.67	29.62	<b>58.66</b>	45.97	30.81	<b>56.90</b>	43.44
PLITS-UniEnc-3B	34.75	28.79	50.79	42.99	31.12	49.71	40.12
PAL-UniEnc-3B(r=3)	<b>37.92</b>	<b>30.70</b>	<b>54.87</b>	<b>47.16</b>	<b>33.53</b>	<b>53.80</b>	<b>43.34</b>

#### 1055 1056 E.4 LAL: PRESERVATION OF TOKEN ORDER INFORMATION 1057

1058 In the standard PLITS integration paradigm, audio tokens are mapped into the LLM input space and  
 1059 physically prepended (or inserted) into the text token sequence. Consequently, the model assigns se-  
 1060 quential position IDs across the entire concatenated sequence—for example,  $[1, \dots, N_{sys}]$  for the sys-  
 1061 tem prompt,  $[N_{sys} + 1, \dots, N_{sys} + N_{audio}]$  for the audio tokens, and  $[N_{sys} + N_{audio} + 1, \dots, N_{total}]$   
 1062 for the user prompt. These position IDs are used by the Rotary Positional Embeddings (RoPE) in  
 1063 the query (Q) and key (K) projections to encode relative and absolute positions, which is crucial for  
 1064 the attention mechanism to function correctly.

1065 In our LAL implementation, audio tokens are not part of the LLM’s input text sequence but are  
 1066 injected directly into the attention mechanism as keys and values. To ensure that the model retains  
 1067 accurate temporal ordering and relative distance information, we explicitly manage the position IDs  
 1068 to mirror the structure of PLITS.

1069 We implement this by adjusting the position IDs of the text tokens to leave a *gap* corresponding to  
 1070 the length of the audio sequence. Specifically, if the system prompt occupies indices  $[1, \dots, k]$ , we  
 1071 do not assign the immediate next integer to the user prompt. Instead, we shift the starting position  
 1072 ID of the user prompt to  $k + N_{audio} + 1$ , effectively reserving the interval  $[k + 1, \dots, k + N_{audio}]$   
 1073 for the audio tokens. Inside the attention module, we assign these reserved position IDs to the audio  
 1074 keys and values as illustrated in Figure 6.

1075 Crucially, this adjustment ensures that for every text token, the position ID used for its Query repre-  
 1076 sentation is identical to the position ID used for its corresponding Key and Value representations. By  
 1077 maintaining this consistency, the model preserves the correct self-attention structure for text while  
 1078 integrating audio context at the appropriate relative positions. We apply equivalent position ID ad-  
 1079 justments in both the Multi-Encoder and Unified-Encoder variants of PAL to maintain token order  
 1080 integrity across all architectures.

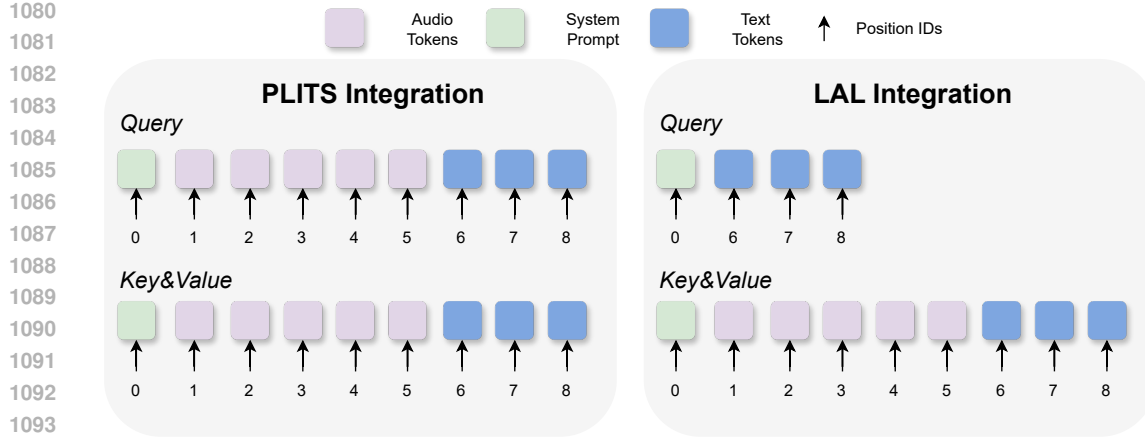


Figure 6: LAL: Preservation of Token Order Information. This diagram illustrates how LAL preserves temporal ordering when integrating audio tokens into the LLM’s attention mechanism. LAL manages position IDs by creating a gap for the audio sequence. By shifting the user prompt’s position ID to  $k + N_{\text{audio}} + 1$ , LAL reserves the interval  $[k + 1, \dots, k + N_{\text{audio}}]$  for audio tokens, ensuring that text token Query, Key, and Value representations maintain identical position IDs and preserve correct self-attention structure.

## E.5 EXTENDED LITERATURE REVIEW

**Audio Representation learning** To obtain rich semantic audio representations, recent advances in audio representation learning have led to powerful audio encoders trained with diverse objectives across different pretraining paradigms. The studies have shifted from simple supervised learning paradigms (Gong et al., 2022a; 2021) to more complex self-supervised paradigms (Huang et al., 2022; Ahmed et al., 2024; Chen et al., 2024; Alex et al., 2025) that employ contrastive objectives and masked-token prediction strategies to capture both global semantic structure and fine-grained local details within audio representations. Furthermore, in the multimodal pretraining paradigm, language-aligned audio representations are obtained through contrastive audio–language models (Elizalde et al., 2023; Wu et al., 2023; Ghosh et al., 2025b) which align the representations of audio and language into a unified semantic space. Transcription-based approaches (Radford et al., 2023) leverage next token prediction on speech-to-text tasks to learn robust audio representations that capture speech semantics and acoustic-linguistic relationships.